Supporting information for

Techno-economic and life-cycle assessment of one-step production of 1,3-butadiene from bioethanol using reaction data under industrial operating conditions

C.E. Cabrera Camacho[†]
Bernabé Alonso-Fariñas[†]
A.L. Villanueva Perales[†*]
F. Vidal-Barrero[†]
Pedro Ollero[†]

[†]Departamento de Ingeniería Química y Ambiental, Escuela Técnica Superior de Ingeniería, Universidad de Sevilla, Camino de los Descubrimientos s/n. 41092 Sevilla, Spain.

Number of pages: 38

Number of figures: 13

Number of tables: 19

Section S1. Supporting Figures and Tables: input data and results of economic and life cycle assessment.

Table S1. Cost factors for estimating direct and indirect costs from purchased equipment cost (PEC) and total installed cost (TIC) [1], respectively.

Direct cost	**PEC (%)**
Purchased equipment cost	100
Purchased equipment installation	39
Instrumentation and control	26
Piping	31
Electrical systems	10
Building (including services)	29
Yard improvements	12
Total direct (installed) costs (TIC)	247
Indirect cost	**TIC (%)**
Engineering and supervision	13.0
Construction expenses	13.8
Legal expenses	1.6
Contractor's fee	7.6
Contingency	15.0
Total indirect costs	51.0

Table S2. Economic assumptions for cash flow analysis.

Parameter	**Value**
Rate of return	10%
Debt/equity	0/100%
Plant lifetime	20 years
Depreciation (linear)	10 years
Salvage value	0
Construction period	1 year
Income tax	30%
Working capital	1-month operating costs
Land	6% TIC

Table S3. Data for estimating OPEX. 8000 operating h/year is assumed.

Fixed operating costs			**% TIC** [1]
Labor			1.56
Maintenance			1.5
General expenses			3.07
Management and operation services			0.44
Cost of goods sold, marketing and logistics			1.32
Insurance			0.5
Total			8.39
Variable operating costs			
<u>Raw materials</u>			
Ethanol[a]	450	€/m^3	Price index[2,3]
Process water[b]	4.61	€/m^3	Correlations [4]
DMF	655.1	€/tonne	AliBaba website[5]
Octane[c]	1.32	€/litre	Average price[6]
Hf-Zn catalyst[d]	83906	€/tonne	Estimated from the cost of catalyst materials[f]
Zeolites[d]	1350	€/tonne	AliBaba website[5]
<u>Utilities</u>			
HPS[b]	47.85	€/tonne	Correlations [4]
MPS[b]	44.78	€/tonne	Correlations [4]
LPS[b]	42.91	€/tonne	Correlations [4]
Cooling water[b]	0.07	€/m^3	Correlations [4]
Chilled water[b]	7.76	€/GJ	Correlations [4]
Refrigerant 1[b]	13.49	€/GJ	Correlations [4]
Refrigerant 2[b]	18.42	€/GJ	Correlations [4]
Electricity[b]	0.18	€/kWh	Correlations [4]
Natural gas[e]	11.54	€/GJ	Price in Spain[7]
<u>Waste management</u>			
Wastewater treatment[b]	1.91	€/m^3	Correlations [4]
Solid disposal[b]	917	€/tonne	Correlations [4]

[a] Average worldwide price of ethanol for the last decade (2008-2018).
[b]Prices estimated using equation of [4] and updated to 2018 price, considering natural gas as fuel source at spanish market price (11.54 €/GJ).
[c]Estimated as gasoline with an average price in Spain.
[d] 50% replacement per year
[e] Based on natural gas lower heating value (LHV). See Table S5.
[f] $HfCl_6$, $Zn(NO_3)_26H_2O$ and SiO_2 bulk costs from AliBaba website [5]

Table S4. Product prices ($€_{2018}$) considered in the economic assessment.

Products	**Value**	**units**	**Reference**
Butenes	599	€/tonne	Estimated [8]
Ethylene	852	€/tonne	Price index[9]
Hydrogen	1960	€/tonne	Estimated [8]
Propylene	1024	€/tonne	Price index[10]
Acetaldehyde (99 wt%)	818	€/tonne	AliBaba website[5]

.

Table S5. Mass and energy balance for each scenario.

	Scenarios		B1	B2	% difference
	Item	**Unit**	**unit/tonne BD**	**unit/tonne BD**	
Inputs	**Total**	tonne	3.800	3.125	-17.8
Raw material	Ethanol (93 wt%)	tonne	3.220	2.690	-16.5
Solvents	Octane	tonne	0.003	0.001	-57.2
	Water	tonne	0.575	0.432	-24.9
	DMF	tonne	0.001	0.001	6.2
Outputs	**Total**	tonne	3.800	3.125	-17.8
Products	1,3-BD	tonne	1.000	1.000	0.0
	Butenes	tonne	0.097	0.062	-36.4
	Ethylene	tonne	0.155	0.197	27.6
	Propylene	tonne	0.054	0.049	-7.6
	Acetaldehyde	tonne	0.127	0.000	---
	Hydrogen	tonne	0.047	0.042	-10.0
To boiler	Residual fuel streams	tonne	0.460	0.235	-48.9
To treatment	Wastewater	tonne	1.861	1.539	-17.3
Utility consumption					
Heating	**Total**	GJ	9.416	10.781	14.5
	HPS	GJ	0.025	3.326	13225.1
	MPS	GJ	0.225	0.093	-58.8
	LPS	GJ	1.325	0.775	-41.6
	Natural gas	GJ	7.841	6.588	-16.0
Cooling	**Total**	GJ	19.693	14.702	-25.3
	Cooling water	GJ	15.926	11.323	-28.9
	Chilled water	GJ	0.227	0.000	---
	Refrigerant 1	GJ	3.347	3.194	-4.6
	Refrigerant 2	GJ	0.193	0.186	-3.9
Electricity		kWh	500.7	344.6	-31.2

[a] Difference calculated as: (B2-B1)*100/B1.
[b]Heating values[11,12]: HPS (250 ºC) = 1720 kJ/kg; MPS (184 ºC) = 2005 kJ/kg; LPS (160 ºC) = 2087 kJ/kg; Natural gas = 47100 kJ/kg.
[c] Cooling values[11,12]: Cooling water (25 ºC) = -83.65 kJ/kg; Chiller (5 ºC) = -41.89 kJ/kg; Refrigerant 1 (-25 ºC)= -407.53 kJ/kg (Propane); Refrigerant 2 (-42 ºC) = -426.23 kJ/kg (Propane).

Table S6. Results of economic evaluation for each scenario (€$_{2018}$) using average market price of ethanol for 2008-2018 (450 €/m^3).

Scenarios	**B1**		**B2**	
OPEX	**Million €/year**	**Share (%)**	**Million €/year**	**Share (%)**
Ethanol	357.4	81.9	298.6	78.2
Catalyst	6.7	1.5	9.3	2.4
Others	3.4	0.8	2.5	0.6
Natural gas	18.1	4.2	15.2	4.0
Hot services	6.6	1.5	22.1	5.8
Cold services	12.8	2.9	11.2	2.9
Electricity	17.8	4.1	12.2	3.2
Waste treatments	1.8	0.4	1.7	0.4
Fixed operating costs	11.8	2.7	9.2	2.4
Total	436.4	100.0	382.0	100.0
Revenues				
1,3-BD	385.5	81.4	344.1	83.6
Butenes	11.7	2.5	7.4	1.8
Ethylene	26.3	5.6	33.6	8.2
Hydrogen	18.2	3.8	16.4	4.0
Propylene	11.0	2.3	10.1	2.5
Acetaldehyde	20.8	4.4	0.0	0.0
Total	473.5	100.0	411.7	100.0
CAPEX (M€)	222.1		179.9	
MBSP (€/tonne)	1927		1721	

Table S7. Inventory for B1 and B2 scenarios.

Scenario	**B1**	**B2**	**Units**
Products	**Amount**	**Amount**	**unit/tonne 1,3-BD**
Avoided products			
Butenes	0.0974	0.0619	tonne
Ethylene	0.1546	0.1973	tonne
Hydrogen	0.0465	0.0419	tonne
Propylene	0.0536	0.0495	tonne
Acetaldehyde	0.1273	0	tonne
Inputs			
Air	17.3	8.9813	tonne
Hafnium	0.0000121	0.0000167	tonne
Materials/fuels			
Ethanol, 93%	3.2202	2.6904	tonne
Water, completely softened	0.5754	0.4319	tonne
N,N-dimethylformamide	0.0009	0.0009	tonne
Natural gas, high pressure	1.0503	0.8825	m^3
Zeolite, powder	0.0051	0.0053	tonne
Petrol, unleaded	0.0032	0.0014	tonne
Hydrogen peroxide, 50%	0.4162	0.1502	tonne
Copper oxide	0.0003	0.0001	tonne
Silica sand	0.000353	0.000487	tonne
Nitric acid, 50%	0.0000721	0.000199	tonne
Zinc	0.0000374	0.0000516	tonne
Chlorine, gaseous	0.00000959	0.0000132	tonne
Carbon black	8.11E-07	0.00000112	tonne
Electricity/heat			
Electricity, medium voltage	1034.05	823.07	kWh
Steam, in chemical industry	0.7618	2.3509	tonne
Water, completely softened	11.4552	7.842	tonne
Outputs			
Emissions to air			
Water	0.9108	0.5577	tonne
Oxygen	2.0756	0.9798	tonne
Nitrogen, atmospheric	13.2669	6.8894	tonne
Carbon dioxide, fossil	0.4588	0.3855	tonne
Carbon dioxide, biogenic	1.2094	0.5438	tonne
Waste to treatment			
Waste zeolite	0.0051	0.0053	tonne
Hazardous waste, for underground deposit	0.0004	0.0006	tonne
Wastewater from vegetable oil refinery	2.4696	1.761	tonne
Wastewater, average, treatment of, capacity 1E9l/year	4.0018	2.6948	m^3

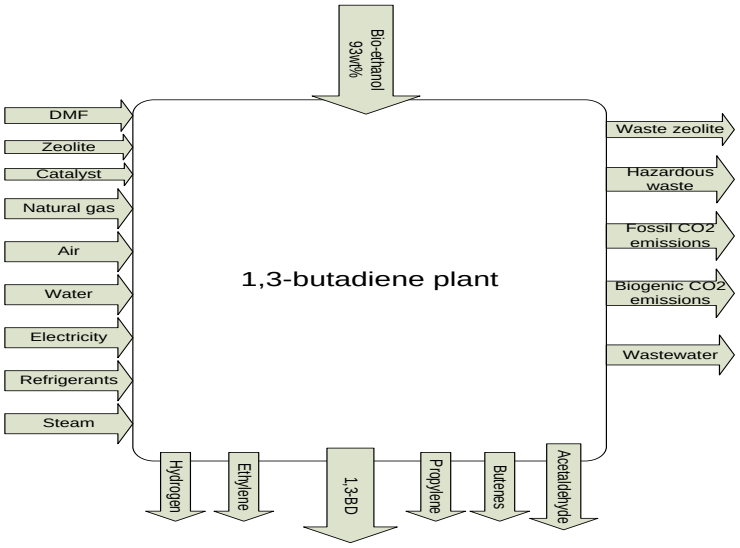

Figure S1. LCA system boundaries of 1,3-BD from bio-ethanol process.

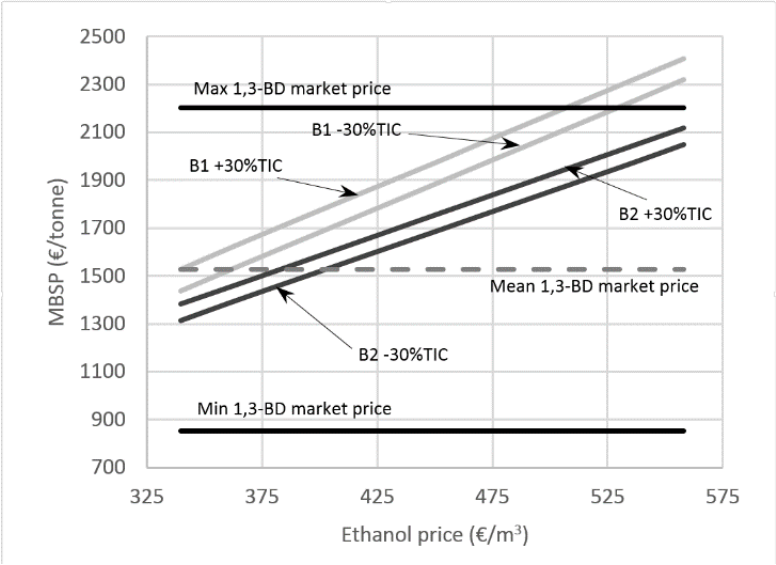

Figure S2. Sensitivity of MBSP to CAPEX and ethanol price.

Section S2: Description of the flowsheet

A more detailed description of the plant is provided based on Figure S3. In the description, the references to the streams, by number or name, are underlined.

Recycled ethanol (29B, 31B) with some impurities (water and by-product) and regenerated ethanol (17) are mixed, vaporized and fed to the catalytic tubes of the furnace reactor. The reactor effluent (1) is cooled to separate the condensable fraction (crude ethanol recycle) (unconverted ethanol, water, acetaldehyde, butanal, acetone, butanol and heavy compounds) from light gases (2) (hydrogen, ethylene, propylene, butenes and 1,3-BD) in Flash-101. Ethanol feed (ethanol with 7 wt% water) is used to absorb 1,3-BD from the light gases together with butenes and light polar compounds (Absorber-T100). Next, 1,3-BD is desorbed from ethanol (T-101), together with butenes and light polar compounds (mainly acetaldehyde), resulting in crude butadiene (8) and regenerated ethanol (7). Acetaldehyde is removed from crude butadiene by washing with water (T-102) and adsorption with molecular sieves (PSA 4A) before extractive distillation with dimethylformamide (DMF), by which butenes are separated from 1,3-BD, obtaining polymer-grade 1,3-BD (99.9 wt% purity and acetaldehyde concentration lower than 10 ppm). On the other hand, the condensable fraction from the reactor (crude ethanol recycle) is sent to a liquid-liquid extraction column (T-103), where heavy compounds are extracted with an organic solvent (octane, HC) so that the subsequent recovery of ethanol by distillation is not hindered by their presence[13]. Water (21B) is also fed to the extraction column to enhance the recovery of ethanol. The organic solvent is regenerated by distillation, (T-104, T-105), separating heavy compounds (25) and recovering some 1,3-BD (22,37) which was dissolved in the crude ethanol recycle. The extracted heavy compounds are used as fuel in the plant while the clean ethanol recycle is sent to a distillation train (T-106, T-107, T-109) where water and other polar compounds are separated from ethanol. As a result of these separations, several streams are obtained: i) purified ethanol recycle (7.5 wt% water); ii) highly pure acetaldehyde stream as co-product iii) a mixture of the rest of separated polar compounds, which is used as fuel in the plant (residual fuel stream from T-109, PSA 3A); iv) water polluted with polar compounds (wastewater from T-106), which is sent to a Fenton process for wastewater treatment.

An effort was made to recover and recycle as much water as possible in order to reduce the consumption of fresh water. Water is used in absorbers T-102 (9B) and T-108 (36B) to remove polar compounds from 1,3-BD. Water from these absorbers (20,38) is regenerated in T-101 and recycled. A fraction of the water from T-102 (21) is not regenerated and used in the extraction of heavy compounds.

Finally, the gas stream from the absorber T-100 (Gases) comprises hydrogen, ethylene and propylene which are separated by means of molecular sieves (PSA 101) and high-pressure distillation (T-111), obtaining high-purity hydrogen, ethylene and propylene streams. These light gases are sold as co-products.

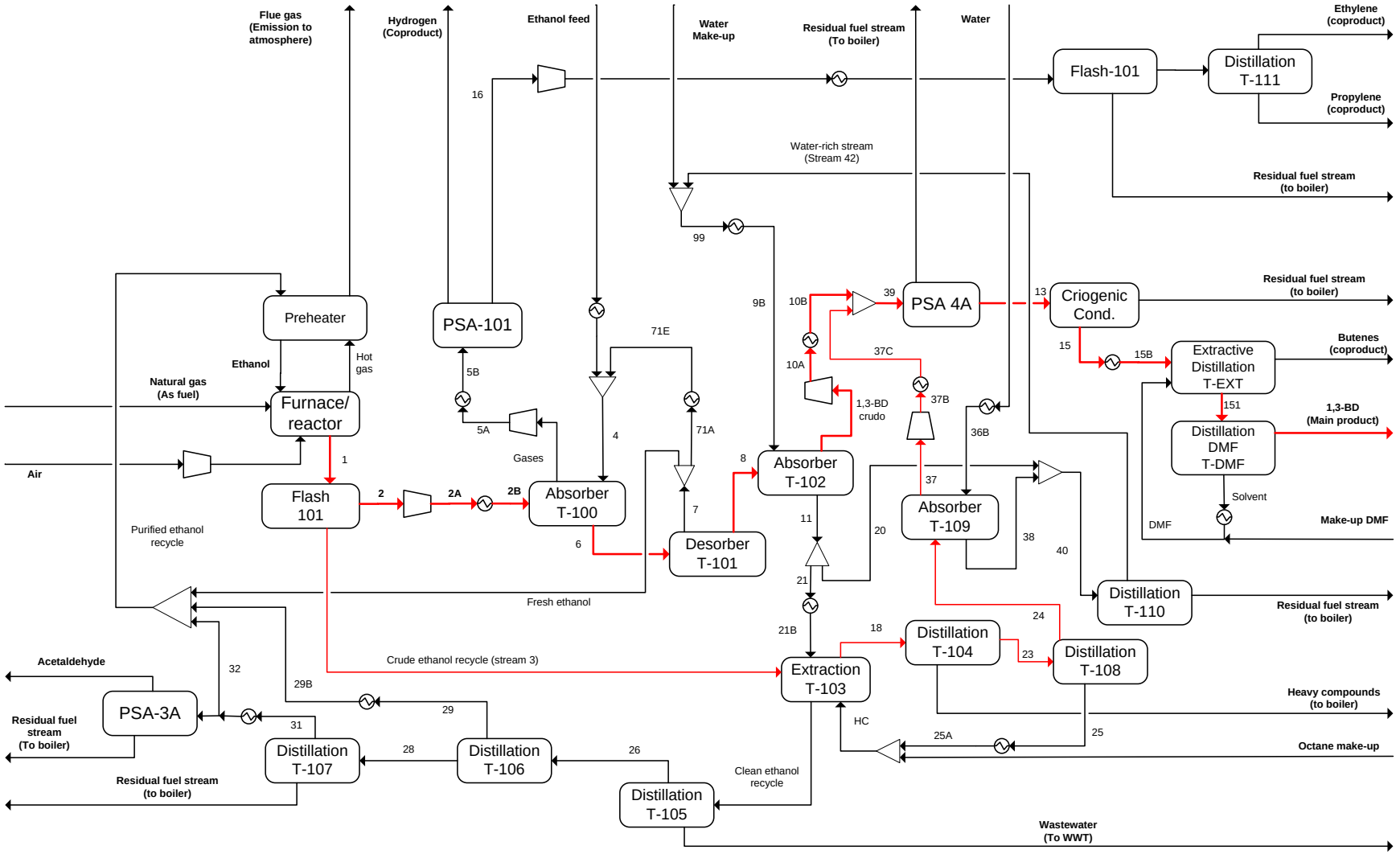

Figure S3. Detailed block diagram. The red arrows depict the flow path for 1,3-BD. Heat integration is omitted for simplicity.

Section S3

Simplified model of the reactor in the production of 1,3-BD from bio-ethanol using the Hf-Zn catalyst.

A simplified model of the synthesis reactor is proposed to predict the mass flow rate of the components in the reactor's outlet stream given the mass flow-rate and composition of the feed to the reactor and the reaction conditions (temperature and space velocity). The following reaction products were considered: 1,3-butadiene, acetaldehyde, water, hydrogen, ethylene, propylene, diethyl ether, 1-butene, 2-trans-butene, n-butanol, n-butanal and dodecane. N-butanal was chosen as the component to lump the numerous light organic compounds observed in the experiments; whereas dodecane was chosen to lump heavy compounds (C_{6+}).

The catalytic reactor was modeled as a mass-yield reactor (Ryield model in Aspen Plus). The mass yield of a component is the mass fraction of the component in the reactor outlet stream. To calculate the mass yields it is necessary to solve the mass balance in the reactor using information from catalyst performance, which is ethanol conversion and carbon selectivity to products and also the conversion of other impurities (polar compounds) present in the ethanol feed. With this information, the molar flow rate of carbon products at the reactor outlet can be calculated and by closing the oxygen and hydrogen atom balances, the molar flow rates of water and hydrogen (non-carbon products) can also be calculated, respectively. The molar flow rates at the reactor outlet are transformed into mass flow rates and then the mass yield is calculated for each component leaving the reactor. At the end of this section, Figure S4 summarizes the algorithm of the reactor model.

The Information on catalyst performance was taken from experimental works. In the first scenario (B1), ethanol conversion and product selectivity from experiments by the authors with hydrous ethanol (7.5 wt% water) were employed as input to the reactor model (Table 1). In the second scenario (B2) operational conditions as well as ethanol conversion and product selectivity were taken from De Baerdemaeker *et al.* [9], who used pure ethanol. Before being used as input in the reactor model, the experimental ethanol conversion and product selectivity were corrected to take into account the water content (7.5 wt%) in the ethanol feed stream to the reactor (see Section S3.1). In both scenarios, a method was implemented in the reactor model to modify the input ethanol conversion and product selectivity in order to take into account the presence of polar compounds in the ethanol feed stream (section S3.2). These corrected ethanol conversion and product selectivity (equations 1 and 2 in section S3.3) were used to solve the mass balance in the reactor.

Section S3.1: Scenario B2. Correcting the effect of water content in ethanol

The experiments reported by De Baerdemaeker *et al.* [14] were conducted with anhydrous ethanol at 360 ºC and WHSV = 0.64 g ethanol*gcat^{-1}h^{-1}. The ethanol conversion and product carbon selectivity were corrected to take into account the water content in the ethanol feed stream to the reactor (7.5 wt%). For that purpose, we estimated the relative change in ethanol conversion and product yield when water content in the ethanol feed increased from 0 to 7.5 wt% at 360 ºC and WHSV = 0.64 g ethanol*gcat^{-1}h^{-1} using experimental data from our catalyst. These relative changes were then applied to the catalyst data reported by De Baerdemaeker *et al.* [14].

The experiments conducted by our group at 360 ºC with anhydrous and hydrous ethanol ranged from WHSV = 1.12 h^{-1}-8 h^{-1}. Therefore, it was necessary to extrapolate the experimental catalyst performance to WSHV= 0.64 h^{-1}. For ethanol conversion the following correlations were obtained at 360 ºC for anhydrous ($X_{ETOH0\%}$) and hydrous ethanol ($X_{ETOH7.5\%}$), as a function of WHSV:

$$X_{ETOH0\%} = 1.00477 - 0.136693(WHSV) + 0.0162544(WHSV)^2 - 0.0007568(WHSV)^3$$

$$X_{ETOH7.5\%} = 0.9339845 - 0.1587462(WHSV) + 0.0201062(WHSV)^2 - 0.0010035(WHSV)^3$$

The relative change in ethanol conversion ($\Delta X_{ETOH/H2O}$) by the presence of water was calculated as follows at WSHV= 0.64 h^{-1}:

$$\Delta X_{ETOH/H2O} = \frac{(X_{ETOH7.5\%} - X_{ETOH0\%})}{X_{ETOH0\%}}$$

As a result, the original fractional ethanol conversion reported by De Baerdemaeker *et al.*[14] (0.988) at 360 ºC and WSHV= 0.64 h^{-1} was corrected as follows:

$$X_{ETOH/H2O} = 0.988(1 + \Delta X_{ETOH/H2O}) = 0.90$$

For each product the correlations for carbon yield were obtained at 360 ºC, for anhydrous ($Y_{ETOH0\%,i}$) and hydrous ($Y_{ETOH7.5\%,i}$) ethanol as a function of WHSV:

$$Y_{ETOH0\%,i} = a_{0,i} + a_{1.i}(WHSV) + a_{2,i}(WHSV)^2 + a_{3,i}(WHSV)^3$$

$$Y_{ETOH7.5\%,i} = a_{0,i} + a_{1,i}(WHSV) + a_{2,i}(WHSV)^2 + a_{3,i}(WHSV)^3$$

The relative changes in yield by the effect of water were calculated by:

$$\Delta Y_i = \frac{(Y_{ETOH7.5\%,i} - Y_{ETOH0\%,i})}{Y_{ETOH0\%,i}}$$

As a result, the original yield values reported by De Baerdemaeker *et al.* [14] were modified as follows:

$$Y_i = Y_{i,original}(1 + \Delta Y_i)$$

The corrected selectivity of each component was calculated as:

$$S_{i,H2O/ETOH} = \frac{Y_i}{X_{ETOH/H2O}}$$

The original and corrected values for product selectivity are shown in Table S8.

Table S8. Original product selectivity reported by [1]De Baerdemaeker *et al*. [14] at 360 ºC, WHSV = 0.64 h^- for anhydrous ethanol and corrected product selectivity for hydrous ethanol (7.5 wt% H_2O).

Component	**Original carbon selectivity ($S_{i,ETOH}$)**	**Corrected carbon selectivity ($S_{i,H2O/ETOH}$)**
Ethylene	0.1000	0.1458
Propylene	0.0360	0.0335
1-Butene	0.0250	0.0206
1,3-BD	0.7000	0.6800
Trans-2-butene	0.0250	0.0206
Acetaldehyde	0.0240	0.0467
Diethyl ether	0.0140	0.0263
Acetone	0.0074	0.0048
Butanal	0.0680	0.0209
Butanol	0.0006	0.0007
Heavies	0.0000	0.0000
Total	1.0000	**1.0000**

Section S3.2. Corrections due to the presence of organic polar compounds in the ethanol feed.

The data obtained by the authors in experiments with the co-feeding of ethanol and polar compounds (acetone, diethyl ether, n-butanal [15,16] and acetaldehyde) were used. Those experiments were carried out at a fixed temperature (360 ºC) and ethanol space velocity (WHSV = 1.12 g ethanol*$gcat^{-1}h^-1$) by varying the inlet concentration of different polar compounds and evaluating the effect on catalyst performance. In our model we roughly assumed that the effect of each polar compound was additive and did not change with operating temperature or space velocity.

Next we present how we modeled the individual effect on the catalyst performance of each polar compound in the ethanol feed and then how the overall effect t was calculated.

a) Acetone (ACTN)

Most of the acetone was converted to heavy compounds by self aldol-condensation reactions; while the rest was converted into propylene by hydrogenation into iso-propanol and further

dehydration. In a large range of acetone concentration in the ethanol feed the overall acetone conversion was very high and acetone did not affect ethanol conversion [15].

$$X_{ACTN} = 0.98$$

$$S_{ACTN-heavy} = \frac{2}{3}$$

$$S_{ACTN-propylene} = \frac{1}{3}$$

b) N-butanal (BTAL)

Most of the n-butanal in ethanol feed was converted into heavy compounds by self aldol-condensation reactions. In a large range of n-butanal concentration in the ethanol feed the overall n-butanal conversion was very high and n-butanal did not affect ethanol conversion [15].

$$X_{BTAL} = 0.97$$

$$S_{heavy} = 1$$

c) Diethyl ether (DEE)

DEE in ethanol feed did not react, nor did it change ethanol conversion, but it did alter its selectivity to ethylene, 1,3-BD and n-butanal according to:

$$\Delta S_{i/DEE} = m_i * x_{DEE}$$

$\Delta S_{i/DEE}$: absolute change in selectivity to compound I by DEE.

x_{DEE}: mass fraction of DEE in the feed reactor (w/w).

The absolute change in selectivity to product i was calculated from experimental data as follows:

$$\Delta S_{i/DEE} = S_{i,0\%DEE} - S_{i,2.5\%DEE}$$

$S_{i,0\%DEE}$: selectivity to i component when DEE concentration in ethanol feed was 0 wt%.

$S_{i,2.5\%DEE}$: selectivity to i component when DEE concentration in ethanol feed was 2.5 wt%.

The m_i parameters are shown in Table S9.

Table S9. Experimental absolute changes in selectivity in the range of 0-2.5wt% of DEE content in the feed and corresponding $m_{i.}$ parameters.

Component	0 w/w	0.025 w/w	m_i
Ethylene	0	0.02880	1.15200
Propylene	0	0.00000	0.00000
1-butene	0	0.00000	0.00000
1,3-butadiene	0	0.00910	0.36400
Trans-2-butene	0	0.00000	0.00000
Acetaldehyde	0	0.00000	0.00000
Diethyl ether	0	0.00000	0.00000
Acetone	0	0.00000	0.00000
Butanal	0	-0.03790	-1.51600
Butanol	0	0.00000	0.00000
Heavies	0	0.00000	0.00000
Total		0.00000	

d) Acetaldehyde (ACTD)

In the experiments were acetaldehyde content in ethanol was changed between (0-10 wt%), we observed that the molar flow rate of acetaldehyde in the product stream was higher than in the feed stream so in absolute terms acetaldehyde was produced in the reactor. Hence, the conversion of inlet acetaldehyde was set to zero. However, the presence of acetaldehyde in the ethanol feed altered the ethanol conversion and selectivity to 1,3-BD, acetaldehyde and n-butanal. The decrease in ethanol conversion and selectivity to acetaldehyde with the inlet concentration of acetaldehyde could be ascribed to the adsorption of acetaldehyde into the Zn-sites which are active for ethanol dehydrogenation. On the other hand, the increase in selectivity to 1,3-BD could be due to the larger concentration of ethanol in the reactor, which favored a rapid conversion of crotonaldehyde from acetaldehyde condensation into crotyl alcohol, a 1,3-BD precursor, by MPV reduction with ethanol. This also showed a tendency to decrease selectivity to other polar compounds (n-butanal).

The change in selectivity is modeled as follows:

$$\Delta S_{i/ACTD} = m_i * x_{ACTD}$$

$\Delta S_{i/ACTD}$: absolute change in selectivity to component i by acetaldehyde.

x_{DEE}: mass fraction of acetaldehyde in the feed reactor (w/w).

The absolute change in selectivity to product i was calculated from experimental data as follows:

$$\Delta S_{i/ACTD} = S_{i,0\%ACTD} - S_{i,10\%ACTD}$$

$S_{i,0\%ACTD}$: selectivity to i component when the concentration of acetaldehyde in ethanol feed was 0 wt%.

$S_{i,10\%ACTD}$: selectivity to i component when the concentration of acetaldehyde in ethanol feed was 10 wt%.

The m_i parameters are shown in Table S10.

Table S10. Experimental absolute changes in selectivity in the range of 0-10 wt% of acetaldehyde content in the feed and corresponding m_i parameters.

Component	**0 w/w**	**0.1w/w**	**m_i**
Ethylene	0	0.00000	0.00000
Propylene	0	0.00000	0.00000
1-Butene	0	0.00000	0.00000
1,3-butadiene	0	0.11045	1.10450
Trans-2-butene	0	0.00000	0.00000
Acetaldehyde	0	-0.06625	-0.44200
Diethyl ether	0	0.00000	0.00000
Acetone	0	0.00000	0.00000
Butanal	0	-0.06625	-0.66250
Butanol	0	0.00000	0.00000
Heavies	0	0.00000	0.00000
Total		**0.00000**	

The change in ethanol conversion by inlet acetaldehyde was calculated with the experimental data shown in Table S11. The relative change in ethanol conversion was calculated as follows:

$$\Delta X_{ETOH/ACTD} = \frac{(X_{0\%ACTD} - X_{w\%ACTD})}{X_{0\%ACTD}}$$

Table S11. Relative change in ethanol conversion in the range of 0-10 wt% of acetaldehyde content in ethanol feed.

Mass fraction of acetaldehyde (w/w)	**Fractional ethanol conversion**	**Relative change in ethanol conversion**
0.0000	0.8706	0.0000
0.0250	0.8275	-0.0520
0.0500	0.7909	-0.1010
0.1000	0.7369	-0.1810

The linear regression of the change in ethanol conversion as a function of acetaldehyde concentration in ethanol feed is:

$$\Delta X_{ETOH/ACTD} = -1.798857 x_{ACTD} - 0.0048$$

$\Delta X_{ETOH/ACTD}$: relative change in ethanol conversion by acetaldehyde.

x_{ACTD}: mass fraction of acetaldehyde in ethanol feed (w/w).

Section S3.3. Overall correction of product selectivity and ethanol conversion by the simultaneous presence of polar compounds in the ethanol feed

The final selectivity of each component i, which takes into account the simultaneous presence of polar compounds in the ethanol feed, was calculated by correcting the input product selectivity ($S_{i,H2O/ETOH}$) and assuming that the effects of the polar compounds are additive:

$$S_{i,f} = S_{i,H2O/ETOH} + \Delta S_{i/DEE} + \Delta S_{i/ACTD} \quad (1)$$

$S_{i,f}$: final selectivity to i component.

$S_{i,H2O/ETOH}$: selectivity to I component for hydrous ethanol feed (7.5 wt% water).

A final ethanol conversion, which takes into account the simultaneous presence of polar compounds in the ethanol feed, was calculated using the following equation:

$$X_{ETOH,f} = X_{ETOH/H2O} + \Delta X_{ETOH/ACTD} \quad (2)$$

$X_{ETOH,f}$: final fractional conversion of ethanol.

$X_{ETOH/H2O}$: input fractional conversion for hydrous ethanol (7.5 wt% water).

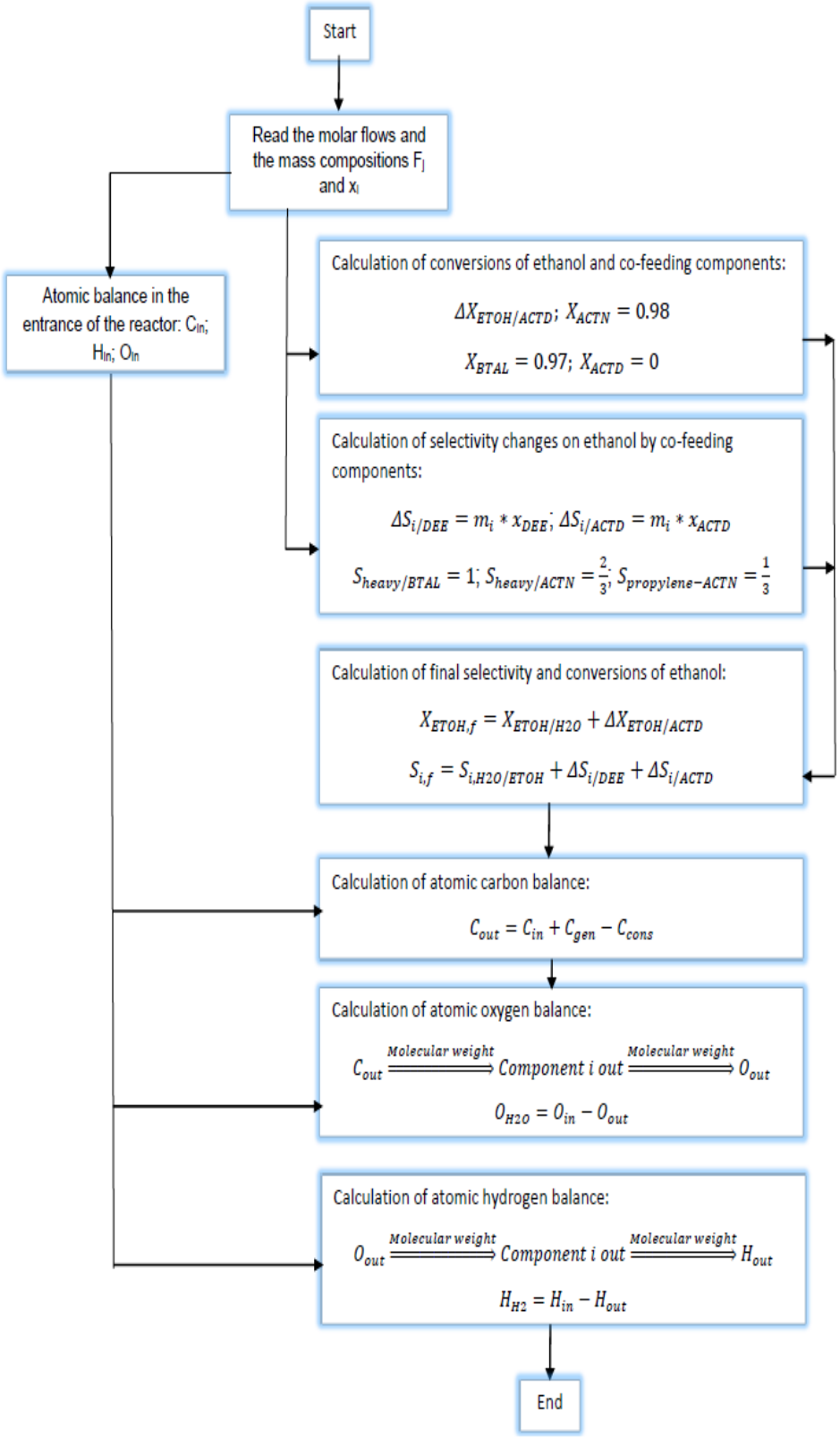

Figure S4. Algorithm of the reactor model.

Section S4. Literature data for uncertainty analysis of environmental impacts.

As explained in section 3.3 of the manuscript, to perform the uncertainty analysis a literature search for impact values related to ethanol production was carried out. For the GWP and WC impact categories, multiple impact values for each type of ethanol (crop and region) were found For the CED impact category, the impact value of ethanol is largely determined by the renewable energy contained in the crop, which is a function on the net heating value of the crop (assumed constant for each crop) and the amount of crop necessary per tonne of ethanol. Therefore, the authors estimated impact values by rescaling the impact value from Ecoinvent V3 with ethanol yields for each of the crops (kg ethanol/kg crop) found in the literature.

Only references from 2000 to the present time were selected, being most of them from 2010 onwards. In the case of USA and Brazil, impacts value for each impact category were searched for 100% corn-based ethanol from the US and 100% sugarcane-based ethanol from Brazil. For Europe, since the representative ethanol is an ethanol mix from different crops (45% from corn, 27% from wheat, 22% from sugar beet and 6% from rye), impact values for ethanol produced in Europe from each of these crops were searched in the literature. Then for each impact category, the distribution of the impact value for the ethanol mix was calculated as all possible combinations of the impact values of each crop-based ethanol weighted by their contribution in the ethanol mix.

Section S4.1 Global Warming Potential (GWP)

The following number (in brackets) of GWP impact values for ethanol were found in the literature:

- Brazil: sugarcane ethanol (21) [17,18,27–31,19–26].
- USA: corn ethanol (18) [18,19,30–33,22–29].
- Europe: sugarbeet ethanol (29)[18,19,37,22,24,27,28,31,34–36] , wheat ethanol (38) [18,19,22,27,28,34–37] , rye ethanol (7) [18,22,31,38,39] , corn ethanol (7) [18,22,34,35] .

The histogram and box plot of the GWP impact values of Brazilian sugarcane ethanol, USA corn ethanol and the European ethanol-mix are shown in Figure S5 and S6, respectively. For the sake of comparison, the median of the impact values from the literature search and the single impact value from Ecoinvent V3 database are compared in Table S12.

Table S12. Comparison of GWP impact values of ethanol production from literature search and Ecoinvent V3, depending on plant location and crop feedstock.

Impact value (kg CO_2/tonne ethanol)	Ecoinvent V3	Literature[a]
Sugarcane (BR)	2570	570
Corn (USA)	1320	1694
Crop mix (EU)	1195	1478
Wheat (EU)	1470 [c]	1450
Sugar beet (EU)	510	1014
Rye (EU)	1530	1030
Corn (EU)	1320[b]	1410

[a]Median value; [b] Not available, assumed corn (USA); [c] Background inventory data for Wheat (EU) taken from Muñoz *et al.* [19] since it is not available in Ecoinvent database.

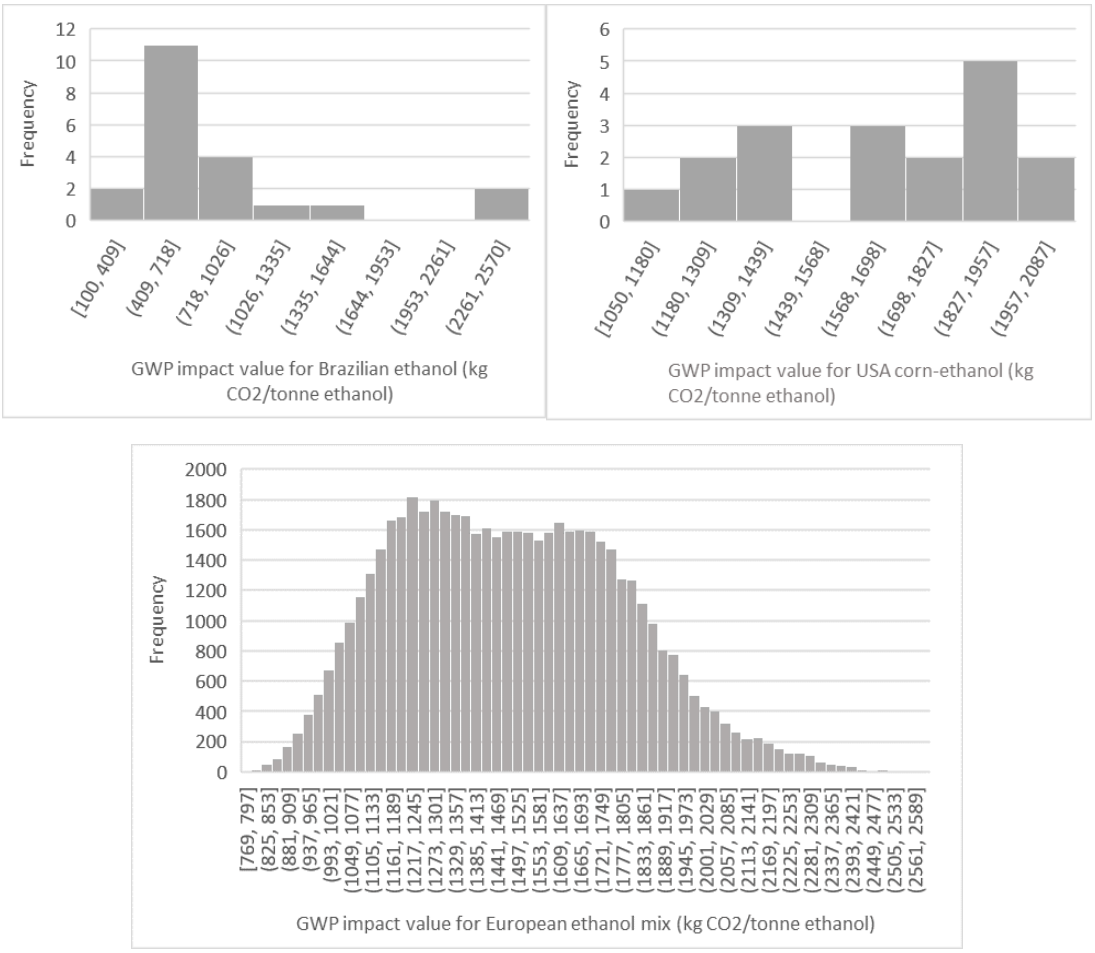

Figure S5. Histogram of GWP impact values based on literature search (Ecoinvent V3 included). Upper-left: Brazilian ethanol. Upper-right: USA corn ethanol. Lower: European ethanol-mix.

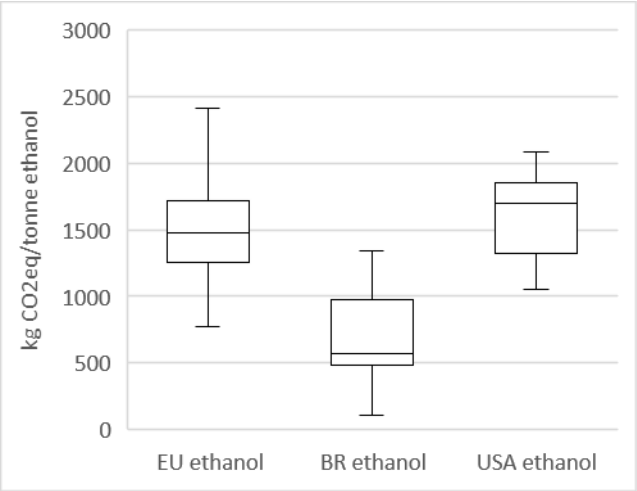

Figure S6. Box plots of GWP impact values for each ethanol source based on literature search (including Ecoinvent V3).

Section S4.2 Water consumption (WC)

The following number (in brackets) of WC impact values for ethanol were found in the literature:

- Brazil: sugarcane ethanol (26) [25,31,40–42].
- USA: corn ethanol (19) [25,31,43,44].
- Europe: sugar beet ethanol (6) [31,43,45,46], wheat ethanol (-), rye ethanol (3) [31,45,46], corn ethanol (7) [31,47].

A small number of impact values were found for European wheat, corn and sugar beet ethanol, which comprise 94% of the European ethanol mix. In order to estimate additional impact values and since most of the water is consumed in the crop cultivation, data of blue water consumed per kg of crop (m^3/tonne crop) and ethanol yield (tonne ethanol/tonne crop) for European wheat, corn and sugar beet were collected from literature. Then, for each of these crops, additional impact values were estimated by fully combining the data of blue water consumption and ethanol yield. This resulted in a total number of 67 impact values for corn ethanol, 64 for wheat ethanol and 156 for sugar-beet ethanol.

For European crops the literature sources for ethanol yield are provided in section S4.3 while those for blue water consumption in crop cultivation are provided next:

- Europe: sugar beet ethanol (10) [48,49], wheat ethanol (4) [48,50,51], corn ethanol (10) [48,49].

The histogram and box plot of the WC impact values of Brazilian sugarcane ethanol, USA corn ethanol and European ethanol-mix are shown in Figure S7 and S8, respectively. For the sake of comparison, the median of the impact values from the literature search and the single impact value from Ecoinvent V3 database are compared in Table S13. A large

discrepancy is observed between the sugar-beet impact value from literature and Ecoinvent database.

Table S13. Comparison of WC impact values of ethanol production from literature search and Ecoinvent V3, depending on plant location and crop feedstock.

Impact value (m^3/tonne ethanol)	Ecoinvent V3	Literature[a]
Sugarcane (BR)	287	81
Corn (USA)	262	121
Crop mix (EU)	164	413
Wheat (EU)	114 [c]	228
Sugar beet (EU)	21	632
Rye (EU)	169	60
Corn (EU)	262[b]	278

[a]Median value; [b] Not available, assumed corn (USA); [c] Background inventory data for Wheat (EU) taken from Muñoz *et al.* [19] since it is not available in Ecoinvent database.

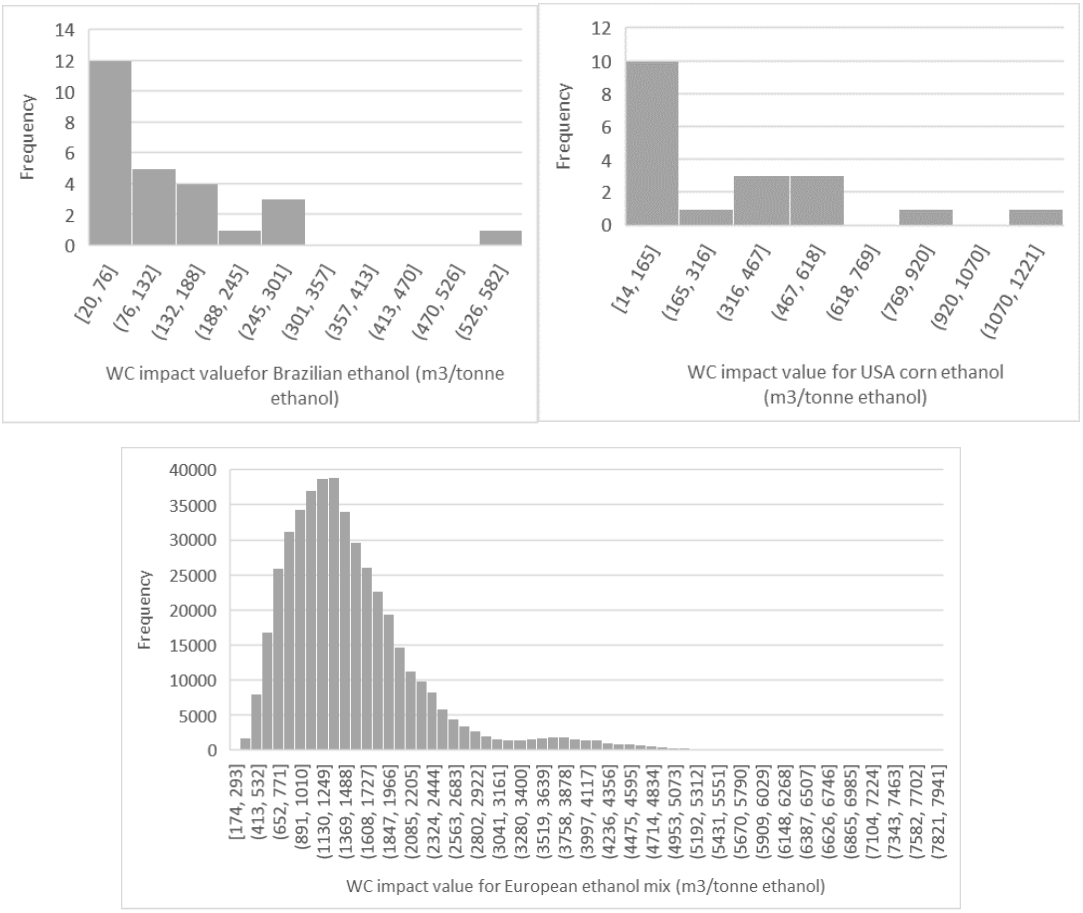

Figure S7. Histogram of WC impact values based on literature search (Ecoinvent V3 included). Upper-left: Brazilian ethanol. Upper-right: USA corn ethanol. Lower: European ethanol mix.

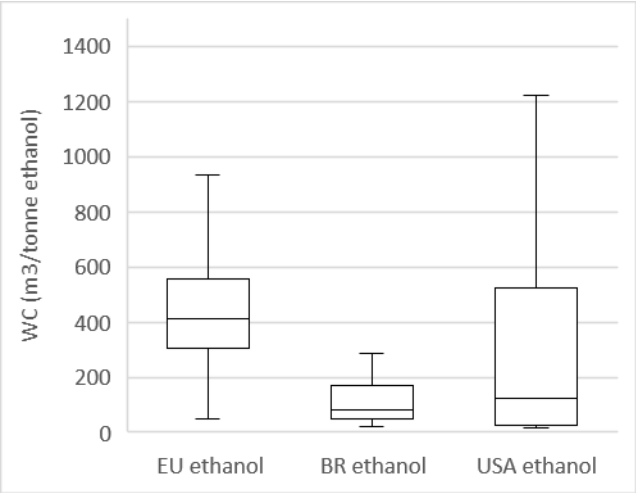

Figure S8. Box plot of WC impact values for each ethanol source based on literature search (including Ecoinvent V3).

Section S4.3 Cumulative energy demand (CED)

The following number (in brackets) of ethanol yields for each crop were found in the literature:

- Brazil: sugarcane (32) [17,18,30,31,42,52–57,19–22,24,25,27,29].
- USA: corn (74) [18,19,55,56,58–62,22,24,25,27,29–32].
- Europe: sugar beet (15) [19,24,64,65,27,31,35,37,46,55,56,63], wheat (15) [19,27,67,29,35,37,46,55,64–66], rye (17) [18,35,46,65], corn (6) [29,31,35,46,65,68].

For each crop-based ethanol, CED ethanol impact values (GJeq/tonne ethanol) were estimated by rescaling the ethanol CED impact value from Ecoinvent database with ethanol yields found in the literature since the CED environmental impact is largely determined by the renewable energy in crop biomass.

The histogram and box plot of the CED impact values of Brazilian sugarcane ethanol, USA corn ethanol and European ethanol-mix are shown in Figure S9 and S10, respectively. For the sake of comparison, the median of the impact values from the literature search and the single impact value from Ecoinvent V3 database are compared in Table S14.

Table S14. Comparison of CED impact values of ethanol from Ecoinvent V3 and those estimated as described in this section, depending on plant location and crop feedstock.

Impact value (GJeq/tonne ethanol)	Ecoinvent V3	Literature[a]
Sugarcane (BR)	77.7	81.3
Corn (USA)	63.2	65.2
Crop mix (EU)	45.4	76.6
Wheat (EU)	83.7	114.7
Sugar beet (EU)	36.4	56.1
Rye (EU)	91.8	91.7
Corn (EU)	63.2[b]	63.2

[a]Median value; [b] Not available, assumed corn (USA); [c] Background inventory data for Wheat (EU) taken from Muñoz *et al.* [19] since it is not available in Ecoinvent database.

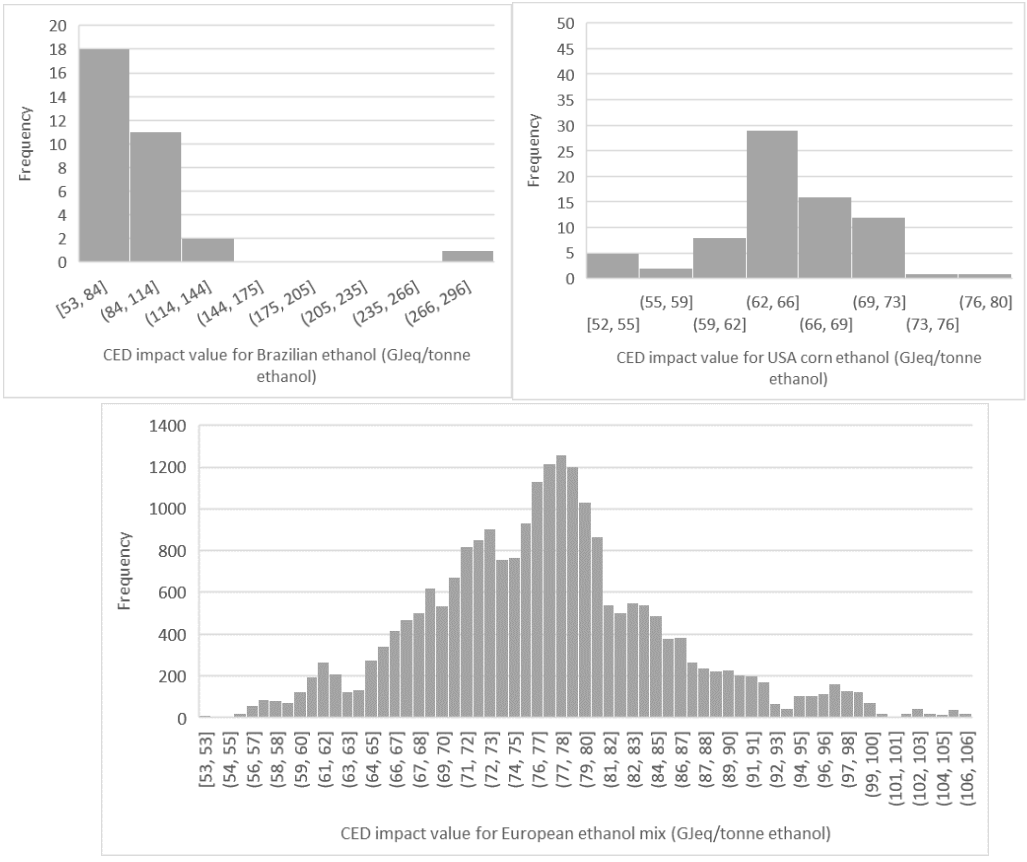

Figure S9. Histogram of WC impact values based on literature search (Ecoinvent V3 included). Upper-left: Brazilian ethanol. Upper-right: USA corn ethanol. Lower: European ethanol mix.

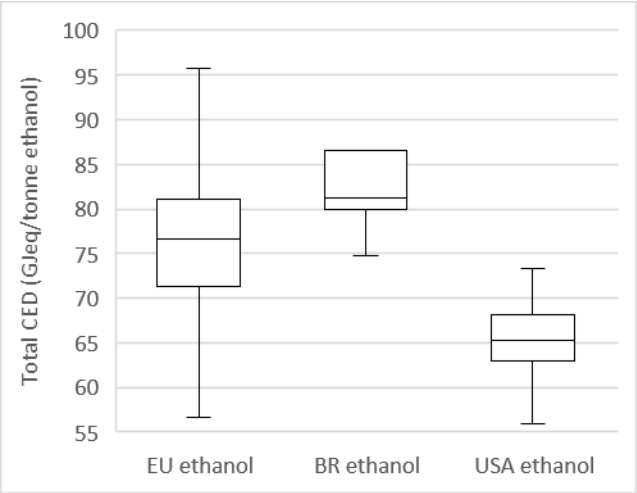

Figure S10. Box plot of CED impact values for each ethanol source based on literature search of ethanol yield for each crop (including Ecoinvent V3).

Section S5. Heat integration methodology and results

The heat integration of the one-step process was done with the tool Aspen Energy Analysis of Aspen Plus V8.8 [69,70], following this procedure: i) extraction of stream data relevant for heat integration from the converged simulation flowsheet to the workspace of Aspen Energy Analysis, ii) calculation of the energy and cost targets by applying pinch analysis and iii) design of the heat exchanger network (HEN) of the plant by solving an optimization problem. Next, the steps of this methodology are explained in more detail. The results for the scenario B1 are presented.

S5.1 Data extraction

First, the simulation flowsheet was prepared for data extraction as explained in [71]. Utilities were preselected in Aspen Plus based on the temperature levels where heat needed to be supplied or removed in the process. Regarding hot utilities, natural gas was selected to supply heat by combustion to the furnace reactor. High, medium and low-pressure steam were selected to satisfy the heat load of the reboilers of the distillation columns. On the other hand, cooling and chilled water were selected to remove heat at moderate temperatures while low-temperature refrigerants were selected for removing heat in some separation operations, such as the cryogenic distillation of propylene and ethylene. Information on these utilities (Table S15) and their prices (Table S3) were specified in Aspen Plus.

Table S15. Temperatures and properties of utilities [12,72,73]

Utility	Inlet temperature (ºC)	Outlet Temperature (ºC)	Sensible heat (kJ/kg)	Latent heat (kJ/kg)
Cold utility				
Cooling water	25	45	-83	---
Chilled water	5	15	-41	---
Propane to -25ºC	-25	-24	---	-407
Propane to -42ºC	-42	-41	---	-426
Hot Utility				
High pressure steam	250	249	---	1720
Medium pressure steam	184	183	---	2005
Low pressure steam	160	159	---	2087
Flue gas (from natural gas combustion)	1200	160	1248	---

An initial HEN was configured where all heat exchangers in the process operated with utilities, i.e, there was not heat integration between process streams. To facilitate the start-up and control of the plant, the reaction heat and the heat for preheating, evaporation and superheating of the ethanol feed to the reactor were not included in the pinch analysis, and fully satisfied by burning natural gas. With this preconfigured HEN the simulation was converged, and the stream data was extracted. Next, a typical minimum temperature approach

(ΔT_{min}) for pinch analysis was chosen (10 °C) [70,72]. With the stream data and ΔT_{min}, Aspen Energy Analysis calculated the energy and operating cost targets by applying pinch analysis, which are shown in Table S16 for scenario B1. Also, the Grand Composite Curve (GCC) was plotted in Aspen Energy Analyzer [74], which allowed investigating the proper selection of utilities.

Table S16. Energy consumption and costs of utilities without heat integration and targets (scenario B1)

	Total utilities		Heating utilities		Cooling utilities	
	No heat integration	Targets	No heat integration	Targets	No heat integration	Targets
Energy consumption (GJ/tonne 1,3-BD)	53.7	32.5	23.6	13.1	30	19.4
Operating costs (Million €/yr)	130.1	62.7	110.7	56.4	19.4	6.2

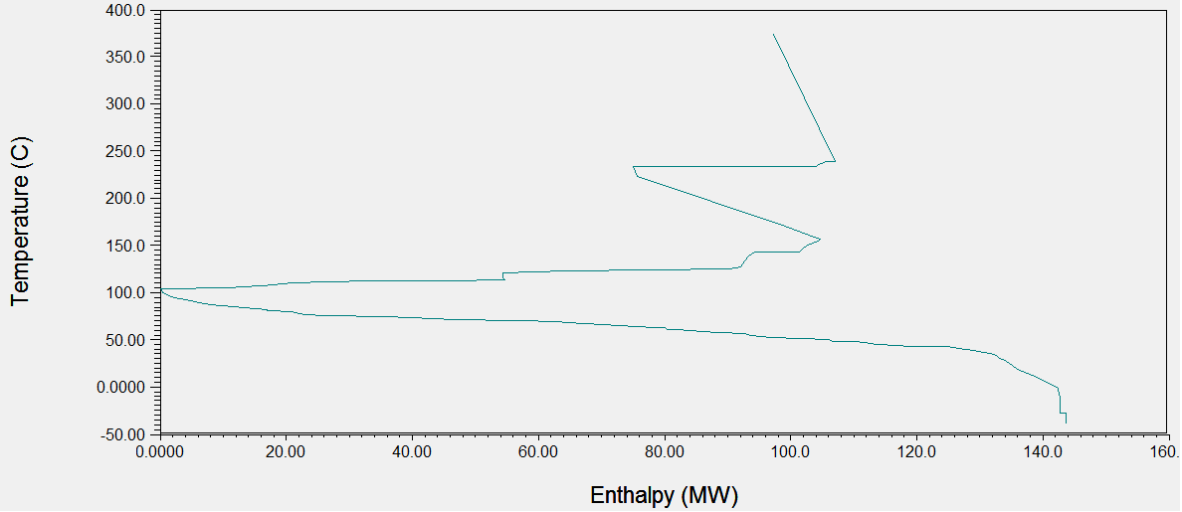

Figure S11. Grand composite curve for B1 scenario.

The shape of the GCC of scenario B1 (Figure S11) is briefly explained next, keeping in mind that the reaction heat and the heat for preheating, evaporation and superheating of the ethanol feed to the reactor are not included. At high temperature there is a surplus of heat from cooling of the reactor effluent. At a shifted temperature close to 250 ºC, a flat region is observed since a high heat load is demanded by the reboilers for regeneration of DMF solvent in the azeotropic distillation of 1,3-BD and octane solvent in the extraction of heavy compounds. Below 250 ºC an excess of heat is available from cooling of the reactor effluent and the hot regenerated DMF solvent. Then, from 150 ºC to the pinch shifted temperature (~105ºC), a flat region is again observed, due to the heat demanded by the reboilers of most of the distillation columns in the plant. The heat to be removed below the pinch is mainly

from the cooling of the reactor effluent down to 40 ºC, and heat to be removed from the condensers of the distillation columns, with some low-temperature cooling needed for the cryogenic distillation of ethylene and propylene and some flash separations.

S5.2 HEN methodology design and results

The HEN was designed by performing a retrofit of an initial HEN, in which the heating or cooling of process streams was fully satisfied with utilities. The procedure applied by Aspen Energy Analysis for retrofitting of the HEN is explained in [75]. Briefly, the first step of the procedure is the selection by the user of a type of HEN modification (addition of a new heat exchanger, relocation or increase in area of an existing heat exchanger). In the second step an optimization algorithm searches the best solutions for a given modification by finding a trade-off between energy costs and heat exchanger capital costs. Aspen Energy Analysis generated ten solutions per requested modification of which the solution with the lowest payback period and/or energy costs was selected. This procedure was repeated until no further modifications were found which reduced the energy costs with a payback lower than 2 years. In the procedure Aspen Energy Analysis calculated the area of the heat exchangers by estimating the heat transfer coefficient of the hot and cold side [70,74] for a shell & tube heat exchanger.

The energy consumption and cost of utilities after the design of the HEN for scenario B1 are shown in Table S17 and S18, respectively. The column "without energetic valorization of residual fuel streams" shows the consumption of utilities when surplus steam generated from combustion of the residual fuel streams of the plant is not accounted for. It is observed that the total consumption of heating and cooling utilities is close to the energy targets shown in Table S16. The consumption of hot utilities (steam) was reduced, as commented before, by burning the residual fuel streams. Therefore, the column "with energetic valorization of residual fuel streams") shows the final consumption of utilities in the one-step process for scenario B1 (excluding natural gas).

Table S17. Consumption of utilities after heat integration (B1 scenario).

Utility consumption			**Without energetic valorization of residual fuel streams**	**With energetic valorization of residual fuel streams**
Heating	**Total**	GJ/tonne 1,3-BD	13.309	1.575
	HPS	GJ/tonne 1,3-BD	3.003	0.025
	MPS	GJ/tonne 1,3-BD	0.225	0.225
	LPS	GJ/tonne 1,3-BD	10.081	1.325
Cooling	**Total**	GJ/tonne 1,3-BD	19.693	19.693
	Cooling water	GJ/tonne 1,3-BD	15.926	15.926
	Chilled water	GJ/tonne 1,3-BD	0.227	0.227
	Refrigerant 1	GJ/tonne 1,3-BD	3.347	3.347
	Refrigerant 2	GJ/tonne 1,3-BD	0.193	0.193

Table S18. Costs of utilities after heat integration (B1 scenario).

Utility consumption			Without energetic valorization of residual fuel streams	With energetic valorization of residual fuel streams
Heating	**Total**	Million €/year	59.2	6.6
	HPS	Million €/year	41.5	5.5
	MPS	Million €/year	1.0	1.0
	LPS	Million €/year	16.7	0.1
Cooling	**Total**	Million €/year	12.8	12.8
	Cooling water	Million €/year	2.7	2.7
	Chilled water	Million €/year	0.4	0.4
	Refrigerant 1	Million €/year	9.0	9.0
	Refrigerant 2	Million €/year	0.7	0.7

The resulting HEN for scenario B1 comprises 24 process-process heat exchangers and 30 utility heat exchangers, with a total area of 24460 m^2 (HEN estimated capital cost: 5.2 million of Euros). Basic information of all heat exchangers is shown in Table S19.

The heat integration of the plant leads to a highly integrated configuration and a brief overview of the HEN is given next. Figure S12 shows a schematic of the heat integration of the reaction area. The heat of the endothermic 1,3-BD reaction is satisfied in the furnace reactor by burning natural gas, and the exiting hot flue gases preheat, evaporate and superheat the reactor ethanol feed (Purified ethanol recycle stream) up to 385 °C, before being vented to the atmosphere at 160 °C. The reactor outlet stream (stream 1A) at 380 °C is the main hot stream above the pinch. It is first cooled in exchanger E-1070 by providing heat to the column bottom stream of the distillation tower T-DMF (tower for recovering 1,3-BD from DMF solvent). The heated bottom stream is then sent to the reboiler of the distillation tower T-DMF. This heat exchange allows to reduce the HP steam consumption of the T-DMF reboiler from 29.1 MW to 18.6 MW. The reactor outlet stream from E-1070 (1B stream) exchanges heat in E-1000 with the column bottom stream (LVT105C) from tower T-105 (see Fig. S3), before being sent to the reboiler of the tower T-105 (Reb-T105). This exchange allows to reduce the LP steam consumption of the Reb-T105 by 9.1 MW. Next, the reactor outlet stream from E-100 (stream 1C) exchanges heat with the column bottom stream (TEXTB) from the extractive distillation tower with DMF (T-EXT), where butenes are separated from 1,3-BD. Finally, the rector outlet stream is cooled down to 40 °C with cooling water before entering the flash separation vessel Flash-101. Figure S13 depicts the rest of the process-process heat exchangers in the plant. Along with the reactor outlet stream, the regenerated DMF solvent at 229 ºC (Bottom T-DMF) is an important hot stream above the pinch, which must be cooled before being recycled to the extractive distillation tower (T-EXT). This stream of DMF exchanges heat with the column bottom stream of T-EXT in E-1010, next, with the column bottom stream of T-106 in E-1020 and next with that of T-105 in E-1050. Finally, the DMF stream is cooled down to 75 °C in E-DMF and recycled to the extractive distillation tower T-DMF.

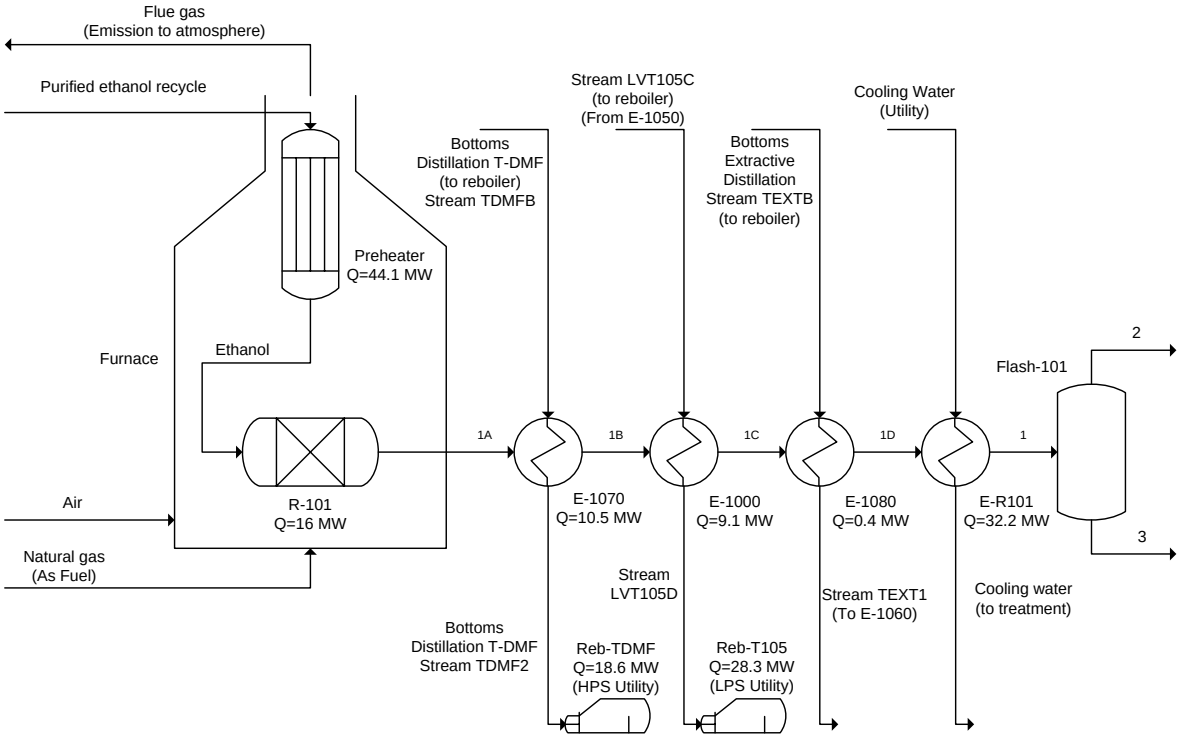

Figure S12. Heat integration in the reaction area, showing heat recovery from the reactor outlet stream (scenario B1).

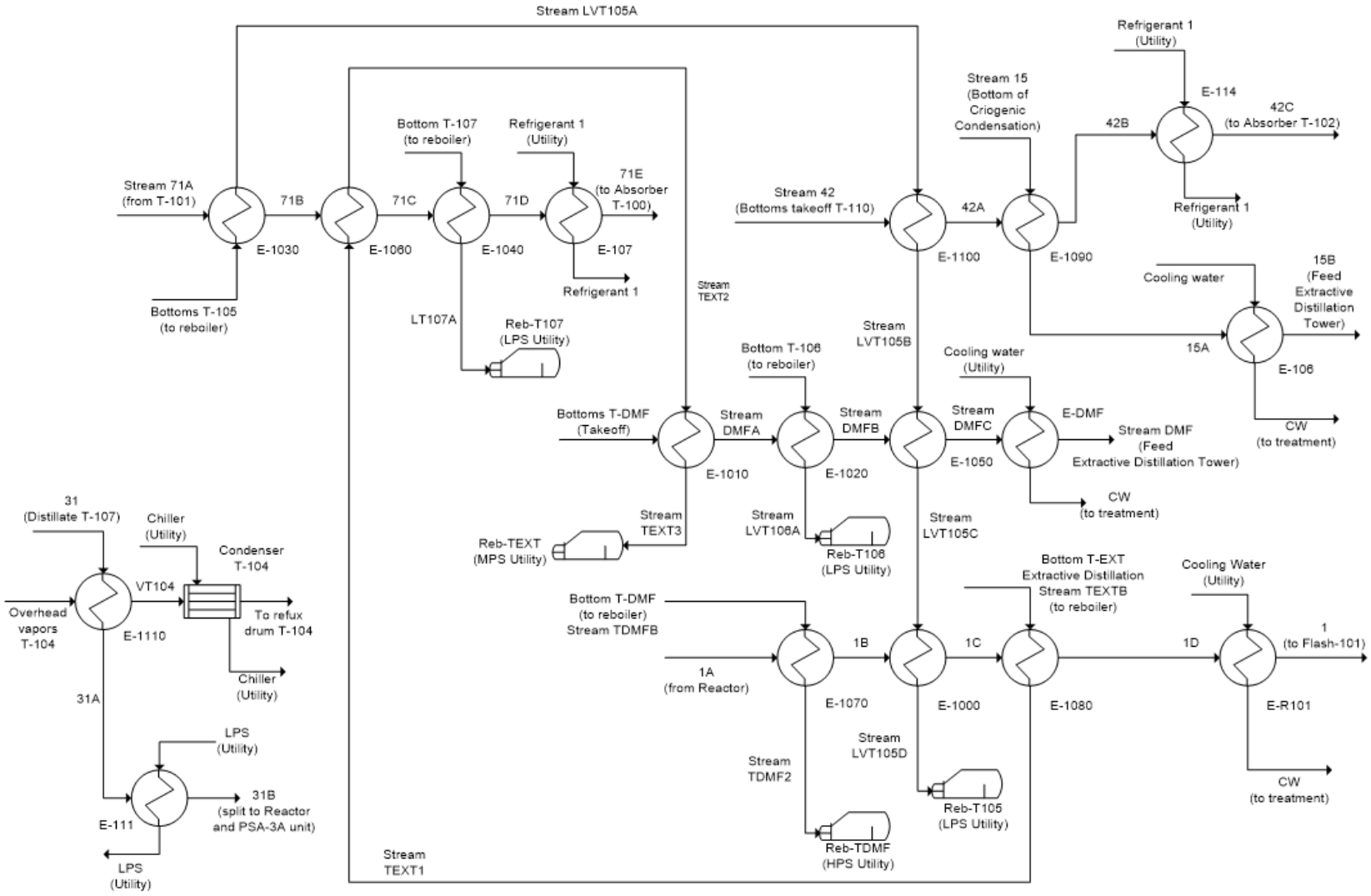

Figure S13. Process-process heat exchangers in the HEN for scenario B1.

Table S19. Heat exchangers of the network for scenario B1. The prefixes COND and REB refer to the condenser and reboiler of the distillation columns shown in Figure S3, respectively.

Exchanger	Hot side (ºC)		Cold side (ºC)		Energy	A
	Thin	Thout	Tcin	Tcout	Q (MW)	m2
CONDT111	-21	-21	-25	-24	1.1	828.2
CONDT101	61	53	25	45	1.8	170.8
CONDT104	119	26	5	15	1.7	93.0
CONDT105	81	62	25	45	43.6	3457.3
CONDT106	63	51	25	45	6.9	746.1
CONDT107	57	53	25	45	1.6	203.1
CONDT108	62	49	25	45	0.1	8.2
CONDT110	79	52	25	45	2.6	177.5
CONDTDMF	51	49	25	45	5.4	772.2
CONDTEXT	51	49	25	45	4.3	612.7
E-100	105	40	25	45	3.4	274.7
E-101	25	5	-25	-24	1.3	65.8
E-102	116	50	25	45	0.5	36.6
E-103	25	5	-25	-24	0.3	13.6
E-104	83	35	25	45	3.5	379.1
E-105	35	-33	-40	-39	1.4	99.1
E-106	160	159	40	40	0.0	0.021
E-107	94	5	-25	-24	19.3	600.9
E-108	156	50	25	45	1.2	27.8
E-109	160	159	36	50	0.3	3.0
E-110	160	159	110	123	0.2	6.7
E-111	184	183	123	123	0.0	0.1
E-113	84	35	25	45	0.1	9.5
E-114	69	5	-25	-24	2.4	86.00
E-115	160	159	26	50	0.0	0.01
E-116	123	80	25	45	0.1	3.31
E-1000	242	106	101	104	9.1	2208
E-1010	229	158	106	153	26.5	840.4
E-1020	158	134	109	109	7.8	444.8
E-1030	123	123	100	100	0.0	0.5
E-1040	100	94	89	96	1.7	712.8
E-1050	134	104	87	101	9.2	757.5
E-1060	123	100	96	106	6.0	1375.1
E-1070	380	242	229	229	10.5	1882.9
E-1080	106	100	96	96	0.4	355.0
E-1090	104	69	-34	40	1.4	35.6

Exchanger	Hot side (ºC)		Cold side (ºC)		Energy	A
	Thin	Thout	Tcin	Tcout	Q (MW)	m2
E-1100	140	104	100	87	1.5	168.62
E-1110	132	119	53	123	1.1	116.4
E-DMF	104	75	25	45	8.6	221.1
E-R101	100	40	25	45	32.2	1521.6
HX-1	112	50	25	45	0.4	13.2
HX-4	160	159	-35	25	0.0	1.1
REB-T111	160	159	58	59	0.5	6.3
REB-T101	160	159	117	122	37.2	1134.9
REB-T104	250	249	230	232	3.3	219.9
REB-T105	160	159	104	108	28.3	647.6
REB-T106	160	159	109	109	0.0	0.03
REB-T107	160	159	96	95	0.0	0.03
REB-T108	184	183	116	155	1.6	44.2
REB-T110	160	159	139	139	7.0	425.7
REB-TDMF	250	249	229	229	18.6	1125.9
REB-TEXT	184	183	153	153	0.0	0.2
Preheater	1127	156	92	385	44.1	1524.8
E-112	25	5	-25	-24	0.1	4.1
Total					**360.11**	**24460**

REFERENCES

[1] Peters M, Timmerhaus K, West R. Plant Design and Economics for Chemical Engineers. New York: McGraw-Hill; 2003.

[2] Markets Insider. Ethanol price commodity. Commodities 2018. https://markets.businessinsider.com/commodities/ethanol-price (accessed February 9, 2019).

[3] U.S. Grains Council. Ethanol Market and Pricing Data. Ethanol, Fuels and Co-Product Pricing 2019. https://grains.org/ethanol_report/ethanol-market-and-pricing-data-february-19-2019/ (accessed March 15, 2019).

[4] Ulrich GD, Vasudevan PT. How to Estimate Utility Costs for a number of utilities. Chem Eng 2006;4:66–9.

[5] Alibaba web page n.d. https://spanish.alibaba.com/ (accessed June 1, 2018).

[6] DieseloGasolina.com. Precio de los carburantes en la Unión Europea 2018. https://www.dieselogasolina.com/precio-de-los-carburantes-con-y-sin-impuestos-en-europa.html (accessed July 20, 2018).

[7] ENDESA. Gas Empresas 2018. https://www.endesaclientes.com/empresas/tarifa-gas-empresas.html (accessed July 20, 2018).

[8] Moncada J, Vural Gursel I, Worrell E, Ramírez A. Production of 1,3-butadiene and ε-caprolactam from C6 sugars: Techno-economic analysis. Biofuels, Bioprod Biorefining 2018;6:246–56. doi:10.1002/bbb.

[9] Waldheim J. Interactive: US May propylene contracts settle up 5 cents/lb on higher spot, upstream. ICIS News 2018. https://www.icis.com/resources/news/2018/05/30/10226350/interactive-us-may-propylene-contracts-settle-up-5-cents-lb-on-higher-spot-upstream/ (accessed July 20, 2018).

[10] Platts. Americas petrochemical outlook H1 2018. Platts Price Index 2018:7. www.platts.com/commodity/petrochemicals (accessed July 20, 2018).

[11] Poling B, Thomson G, Friend D, Rowley R, Wilding V. Section 2: Physical and Chemical Data. In: Green D, Perry R, editors. Perry's Chem. Eng. Handb. 8th ed., McGraw-Hill; 2008, p. 2–47.

[12] NIST. Chemistry WebBook NIST 2016. http://webbook.nist.gov/chemistry/ (accessed Jan 8, 2018)

[13] Dastillung R, Fischer B, Jacquin M, Huy-Ghe R. Procédé de production de butadiène et d'hydrogène à partir d'éthanol en deux étapes réactionnelles à faible consommation en eau et en énergie. WO2016042096A1, 2016.

[14] De Baerdemaeker T, Feyen M, Müller U, Yilmaz B, Xiao FS, Zhang W, et al. Bimetallic Zn and Hf on silica catalysts for the conversion of ethanol to 1,3-butadiene. ACS Catal 2015;5:3393–7. doi:10.1021/acscatal.5b00376.

[15] Cabello González GM, Murciano R, Villanueva Perales AL, Martínez A, Vidal-Barrero F, Campoy M. Ethanol conversion into 1,3-butadiene over a mixed Hf-Zn catalyst: A study of the reaction pathway and catalyst deactivation. Appl Catal A Gen 2019;570:96–106. doi:10.1016/j.apcata.2018.11.010.

[16] Cabello González GM, Concepción P, Villanueva Perales AL, Martínez A, Campoy M, Vidal-Barrero F. Ethanol conversion into 1,3-butadiene over a mixed Hf-Zn catalyst: Effect of reaction conditions and water content in ethanol. Fuel Process Technol 2019;193:263–73. doi:10.1016/j.apcata.2018.11.010.

[17] Macedo IC, Lima Verde Leal MR, Azevedo Ramos da Silva JE. Assessment of greenhouse gas emissions in the production and use of fuel ethanol in Brazil. Government of the State of São Paulo.2004.
[18] Jungbluth N, Chudacoff M, Dauriat A, Dinkel F, Doka G, Faist Emmenegger M, et al. Life Cycle Inventories of Bioenergy. Ecoinvent Report No. 17. Dübendorf-Switzerland: 2007.
[19] Muñoz I, Flury K, Jungbluth N, Rigarlsford G, Milà L, King H. Life cycle assessment of bio-based ethanol produced from different agricultural feedstocks. Int J Life Cycle Assess 2013:1–11. doi:10.1007/s11367-013-0613-1.
[20] Macedo IC, Seabra JEA, Silva JEAR. Green house gases emissions in the production and use of ethanol from sugarcane in Brazil: The 2005/2006 averages and a prediction for 2020. Biomass and Bioenergy 2008;32:582–95. doi:10.1016/j.biombioe.2007.12.006.
[21] Seabra JEA, Macedo IC, Chum HL, Faroni CE, Sarto CA. Life cycle assessment of Brazilian sugarcane products: GHG emissions and energy use Joaquim. Biofuels, Bioprod Biorefining 2012;6:246–56. doi:10.1002/bbb.
[22] Edwards R, Larivé J-F, Rickeard D, Weindorf W. Well-to-tank Report Version 4.a. JEC Well-to-Wheels Analysis of Future Automotive Fuels and Powertrains in the European Context. 2014.
[23] Wang M, Han J, Dunn JB, Cai H, Elgowainy A. Well-to-wheels energy use and greenhouse gas emissions of ethanol from corn, sugarcane and cellulosic biomass for US use. Environ Res Lett 2012;7:1–13. doi:10.1088/1748-9326/7/4/045905.
[24] Manochio C, Andrade BR, Rodriguez RP, Moraes BS. Ethanol from biomass: A comparative overview. Renew Sustain Energy Rev 2017;80:743–55. doi:10.1016/j.rser.2017.05.063.
[25] Mekonnen MM, Romanelli TL, Ray C, Hoekstra AY, Liska AJ, Neale CMU. Water, Energy, and Carbon Footprints of Bioethanol from the U.S. and Brazil. Environ Sci Technol 2018;52:14508–18. doi:10.1021/acs.est.8b03359.
[26] De Oliveira MD. Sugarcane and ethanol production and carbon dioxide balances. In: Pimentel D, editor. Biofuels, Sol. Wind as Renew. Energy Syst. Benefits Risks, Springer Science+Business Media B.V.; 2008, p. 215–30. doi:10.1007/978-1-4020-8654-0_9.
[27] Roy P, Dutta A. Life Cycle Assessment (LCA) of Bioethanol Produced From Different Food Crops: Economic and Environmental Impacts. Elsevier Inc.; 2019. doi:10.1016/b978-0-12-813766-6.00019-9.
[28] Pacheco R, Silva C. Global warming potential of biomass-to-ethanol: Review and sensitivity analysis through a case study. Energies 2019;12. doi:10.3390/en12132535.
[29] Pereira LG, Cavalett O, Bonomi A, Zhang Y, Warner E, Chum HL. Comparison of biofuel life-cycle GHG emissions assessment tools: The case studies of ethanol produced from sugarcane, corn, and wheat. Renew Sustain Energy Rev 2019;110:1–12. doi:10.1016/j.rser.2019.04.043.
[30] Dias De Oliveira ME, Vaughan BE, Rykiel EJ. Ethanol as Fuel: Energy, Carbon Dioxide Balances, and Ecological Footprint. Bioscience 2005;55:593. doi:10.1641/0006-3568(2005)055[0593:eafecd]2.0.co;2.
[31] Ecoinvent Centre. Ecoinvent V3 Database. 2018.
[32] Liska AJ, Yang HS, Bremer VR, Klopfenstein TJ, Walters DT, Erickson GE, et al.

Improvements in life cycle energy efficiency and greenhouse gas emissions of corn-ethanol. J Ind Ecol 2009;13:58–74. doi:10.1111/j.1530-9290.2008.00105.x.
[33] Shylesh S, Gokhale AA, Scown CD, Kim D, Ho CR, Bell AT. From Sugars to Wheels: The Conversion of Ethanol to 1,3-Butadiene over Metal-Promoted Magnesia-Silicate Catalysts. ChemSusChem 2016;9:1462–72. doi:10.1002/cssc.201600195.
[34] ADEME. Life Cycle Analyses Applied to First Generation Biofuels Used in France. 2010.
[35] Biograce. BIOGRACE-Harmonised Calculations of Biofuel Greenhouse Gas Emissions in Europe. 2015. https://www.biograce.net/home (accessed January 20, 2020).
[36] Mortimer ND, Elsayed MA, Horne RE. Energy and Greenhouse Gas Emissions for Bioethanol Production from Wheat Grain and Sugar Beet. Sheffield Hallam University: 2004.
[37] Weinberg J, Kaltschmitt M. Greenhouse gas emissions from first generation ethanol derived from wheat and sugar beet in Germany - Analysis and comparison of advanced by-product utilization pathways. Appl Energy 2013;102:131–9. doi:10.1016/j.apenergy.2012.06.047.
[38] Ahlgren S, Hansson P-A, Kimming M, Aronsson P, Lundkvist H. Greenhouse gas emissions from cultivation of agricultural crops for biofuels and production of biogas from manure. Swedish University of Agricultural Sciences 2011.
[39] Astover A, Shanskiy M, Lauringson E. Development and application of the methodology for the calculation of average greenhouse gas emissions from the cultivation of rapeseed, wheat, rye, barley and triticale in Estonia. Estonian University of Life Sciences, Institute of Agricultural and Environmental Sciences. Tartu: 2015.
[40] Dourado Hernandes TA, Bof Bufon V, Seabra JEA. Water footprint of biofuels in Brazil: assessing regional differences. Biofuels, Bioprod Biorefining 2012;6:246–56. doi:10.1002/bbb.
[41] Chico D, Santiago AD, Garrido A. Increasing efficiency in ethanol production: Water footprint and economic productivity of sugarcane ethanol under nine different water regimes in north-eastern Brazil. Spanish J Agric Res 2015;13:1–10. doi:10.5424/sjar/2015132-6057.
[42] Tsiropoulos I, Faaij APC, Seabra JEA, Lundquist L, Schenker U, Briois JF, et al. Life cycle assessment of sugarcane ethanol production in India in comparison to Brazil. Int J Life Cycle Assess 2014;19:1049–67. doi:10.1007/s11367-014-0714-5.
[43] Dominguez-Faus R, Powers SE, Burken JG, Alvarez PJ. The water footprint of biofuels: A drink or drive issue? Environ Sci Technol 2009;43:3005–10. doi:10.1021/es802162x.
[44] Teter J, Yeh S, Khanna M, Berndes G. Water impacts of U.S. biofuels: Insights from an assessment combining economic and biophysical models. PLoS One 2018;13:1–22. doi:10.1371/journal.pone.0204298.
[45] Gerbens-Leenes PW. Bioenergy water footprints, comparing first, second and third generation feedstocks for bioenergy supply in 2040. Eur Water 2017:373–80.
[46] Mekonnen MM, Hoekstra AY. The green, blue and grey water footprint of crops and derived crop products. Hydrol Earth Syst Sci 2011;15:1577–600. doi:10.5194/hess-15-1577-2011.

[47] Gerbens-Leenes PW, Hoekstra Y. The water footprint of sweeteners and bio-ethanol from sugarcane, sugar beet and maize. Value of Water Research Report Series, No 38. Delft, Netherlands: 2009.
[48] Thaler S, Gobin A, Eitzinger J. Water footprint of main crops in Austria. Bodenkultur 2017;68:1–15. doi:10.1515/boku-2017-0001.
[49] Gobin A, Kersebaum KC, Eitzinger J, Trnka M, Hlavinka P, Takáč J, et al. Variability in the water footprint of arable crop production across European regions. Water (Switzerland) 2017;9. doi:10.3390/w9020093.
[50] Kersebaum KC, Kroes J, Gobin A, Takáč J, Hlavinka P, Trnka M, et al. Assessing uncertainties of water footprints using an ensemble of crop growth models on winter wheat. Water (Switzerland) 2016;8. doi:10.3390/w8120571.
[51] Tuninetti M, Tamea S, D'Odorico P, Laio F, Ridolfi L. Global sensitivity of high-resolution estimates of crop water footprint. Water Resour Res 2015;51:8257–72. doi:10.1002/2015WR017148.
[52] Goldemberg J, Guardabassi P. The potential for fi rst- generation ethanol production from sugarcane. Biofuels, Bioprod Biorefining 2010;4:17–24. doi:10.1002/bbb.
[53] Lisboa CC, Butterbach-Bahl K, Mauder M, Kiese R. Bioethanol production from sugarcane and emissions of greenhouse gases - known and unknowns. GCB Bioenergy 2011;3:277–92. doi:10.1111/j.1757-1707.2011.01095.x.
[54] Nicula de Castro RE, de Brito Alves RM, Oller do Nascimento CA, Giudici R. Assessment of Sugarcane-Based Ethanol Production. IntechOpen 2012;i:1–21. doi:10.1016/j.colsurfa.2011.12.014.
[55] Rajagopal, Deepak and Zilberman, David, Review of Environmental, Economic and Policy Aspects of Biofuels (September 1, 2007). World Bank Policy Research Working Paper No. 4341. https://ssrn.com/abstract=10124732007. (accessed March 27, 2020)
[56] Berg C. World Fuel Ethanol Analysis and Outlook. Online Distill Netw Distill Fuel Ethanol Plants Worlwide 2004. https://www.distill.com/World-Fuel-Ethanol-A&O-2004.html (accessed March 27, 2020).
[57] Macedo IC, Seabra JEA. Chapter 4. Mitigation of GHG emissions using sugarcane bioethanol. In: Zuurbier P, Van de Vooren J, editors. Sugarcane Ethanol. Contrib. to Clim. Chang. Mitig. Environ., Wageningen Academic Publishers; 2008, p. 95–110.
[58] Wu M. Analysis of the Efficiency of the U.S. Ethanol Industry 2007. AUS Dept Energy Lab - Chicago Illlinois 2008:1–7.
[59] Flugge M, Lewandrowski J, Rosenfeld J, Boland C, Hendrickson T, Jaglo K, et al. A Life-Cycle Analysis of the Greenhouse Gas Emissions of Corn-Based Ethanol. Report prepared by ICF under USDA Contract No. AG-3142-D-16-0243. January 30, 2017 2017.
[60] Lewandrowski J, Rosenfeld J, Pape D, Hendrickson T, Jaglo K, Moffroid K. The greenhouse gas benefits of corn ethanol–assessing recent evidence. Biofuels 2019;11:361–75. doi:10.1080/17597269.2018.1546488.
[61] Han J, Tao L, Wang M. Well-to-wake analysis of ethanol-to-jet and sugar-to-jet pathways. Biotechnol Biofuels 2017;10:1–15. doi:10.1186/s13068-017-0698-z.
[62] Mohanty SK, Swain MR. Bioethanol Production From Corn and Wheat: Food, Fuel, and Future. Elsevier Inc.; 2019. doi:10.1016/b978-0-12-813766-6.00003-5.
[63] Henke S, Bubník Z, Hinková A, Pour V. Model of a sugar factory with bioethanol production in program Sugars™. J Food Eng 2006;77:416–20.

doi:10.1016/j.jfoodeng.2005.07.007.
[64] Elsayed MA, Matthews R, Mortimer ND. Carbon and Energy Balances for a Range of Biofuels Options. Sheffield Hallam University: 2004.
[65] Edwards R, Mulligan D, Giuntoli J, Agostini A, Boulamanti A, Koeble R, et al. Part Three-Liquid Biofuels Processes and Input Data. JRC Sci. Policy Reports-Assessing GHG Default Emiss. from Biofuels EU Legis., Ispra: European Commission Joint Research Centre Institute for Energy and Transport; 2011, p. 123–62.
[66] Ahlgren S, Röös E, Di Lucia L, Sundberg C, Hansson PA. EU sustainability criteria for biofuels: Uncertainties in GHG emissions from cultivation. Biofuels 2012;3:399–411. doi:10.4155/bfs.12.33.
[67] Belboom S, Bodson B, Léonard A. Does the production of Belgian bioethanol fit with European requirements on GHG emissions? Case of wheat. Biomass and Bioenergy 2015;74:58–65. doi:10.1016/j.biombioe.2015.01.005.
[68] Franceschin G, Zamboni A, Bezzo F, Bertucco A. Ethanol from corn: a technical and economical assessment based on different scenarios. Chem Eng Res Des 2008;86:488–98. doi:10.1016/j.cherd.2008.01.001.
[69] Aspen Technology Inc. Aspen Plus V8.8. 2015.
[70] Aspen Technologies. Getting Started with Activated Energy Analysis in Aspen Plus. https://esupport.aspentech.com/ (accessed January 8, 2018).
[71] Zhang J, Brownrigg R. Prepare a Flowsheet for Energy Analysis in Aspen Plus and Aspen HYSYS: An industry white paper. Aspen Technology 2013.
[72] Kemp IC. Pinch Analysis and Process Integration. 2nd ed., Elsevier; 2007.
[73] Poling B, Thomson G, Friend D, Rowley R, Wilding V. Section 2: Physical and Chemical Data. In: Green D, Perry R, editors. Perry's Chem. Eng. Handb. 8th ed., McGraw-Hill; 2008, p. 2–47.
[74] Aspen Technology Inc. Aspen Energy Analyzer-User Guide V8.8. 2015.
[75] Asante NDK, Zhu XX. An automated and interactive approach for heat exchanger network retrofit. Trans IChemE 1997;75;349-60. doi:10.1205/026387697523660